

RGS proteins reconstitute the rapid gating kinetics of $G\beta\gamma$ -activated inwardly rectifying K^+ channels

CRAIG A. DOUPNIK*, NORMAN DAVIDSON†, HENRY A. LESTER‡, AND PAULO KOFUJI

Division of Biology 156–29, California Institute of Technology, Pasadena, CA 91125

Contributed by Norman Davidson, July 17, 1997

ABSTRACT G protein-gated inward rectifier K^+ (GIRK) channels mediate hyperpolarizing postsynaptic potentials in the nervous system and in the heart during activation of $G\alpha(i/o)$ -coupled receptors. In neurons and cardiac atrial cells the time course for receptor-mediated GIRK current deactivation is 20–40 times faster than that observed in heterologous systems expressing cloned receptors and GIRK channels, suggesting that an additional component(s) is required to confer the rapid kinetic properties of the native transduction pathway. We report here that heterologous expression of “regulators of G protein signaling” (RGS proteins), along with cloned G protein-coupled receptors and GIRK channels, reconstitutes the temporal properties of the native receptor → GIRK signal transduction pathway. GIRK current waveforms evoked by agonist activation of muscarinic m_2 receptors or serotonin 1A receptors were dramatically accelerated by co-expression of either RGS1, RGS3, or RGS4, but not RGS2. For the brain-expressed RGS4 isoform, neither the current amplitude nor the steady-state agonist dose-response relationship was significantly affected by RGS expression, although the agonist-independent “basal” GIRK current was suppressed by $\approx 40\%$. Because GIRK activation and deactivation kinetics are the limiting rates for the onset and termination of “slow” postsynaptic inhibitory currents in neurons and atrial cells, RGS proteins may play crucial roles in the timing of information transfer within the brain and to peripheral tissues.

Regulators of G protein signaling (RGS proteins) are members of a novel multigene family (1–3) that accelerate the GTPase rate of heterotrimeric $G\alpha(i/o)$ proteins through direct interaction (4–6). These GTPase-activating proteins (GAPs) have generated recent interest because of well-established discrepancies between the *in vitro* GTPase rate of purified $G\alpha$ subunits and the much greater (typically >40 -fold) *in vivo* rate at which some G protein-mediated signals are terminated (7). For instance, in the G protein signaling cascade of visual phototransduction (8, 9), RGS proteins may help to produce the rapid signal termination necessary for processing visual stimuli at a high temporal resolution (10).

An analogous kinetic discrepancy exists for the $G\beta\gamma$ -activated inward rectifier K^+ (GIRK) channel in atrial myocytes (11, 12). Muscarinic m_2 receptor-activated GIRK currents deactivate after agonist washout ≈ 40 -fold faster ($1/\tau_{\text{deact}} \approx 2 \text{ s}^{-1}$) than the GTP hydrolysis rate of pertussis toxin-sensitive $G\alpha$ subunits ($k_{\text{cat}} \approx 0.05 \text{ s}^{-1}$). Yet these $G\alpha(i/o)$ subunits are thought to terminate the current by resequencing $G\beta\gamma$ dimers after returning to their GDP-bound state (12). GIRK channels expressed in CA3 hippocampal neurons display a similar rapid deactivation (13). However, cloned GIRK channels expressed in *Xenopus* oocytes with the m_2 receptor

deactivate with a rate constant that is nearly equivalent ($\approx 0.05 \text{ s}^{-1}$) to the intrinsic $G\alpha$ subunit GTPase rate constant (14). Thus, atrial myocytes and hippocampal neurons, but not *Xenopus* oocytes, may express one or more GAPs that accelerate GIRK kinetics. The slowing of atrial GIRK current deactivation in excised membrane patches provides additional evidence for an extrinsic GAP-like component (15).

Here we demonstrate that when cloned GIRK channels and the muscarinic m_2 receptor are coexpressed with certain RGS proteins in *Xenopus* oocytes or Chinese hamster ovary (CHO) cells, receptor-evoked GIRK current kinetics are accelerated and mimic the properties of GIRK currents in native atrial myocytes and hippocampal neurons. These results suggest that endogenous RGS proteins in atrial myocytes and neurons are important factors that affect the temporal gating properties of GIRK channels. Moreover, RGS proteins accelerated the GIRK activation phase as well as the deactivation phase without affecting the EC_{50} value for activation by acetylcholine (ACh), raising new mechanistic questions regarding the interplay of receptors, $G\beta\gamma$ dimers, $G\alpha$ subunits, and RGS proteins in GIRK channel gating. The physiological implications of these findings are that RGS proteins may determine the timing, amplitude, and duration of GIRK-mediated “slow” inhibitory synaptic transmission in the nervous system.

MATERIALS AND METHODS

RGS cDNAs. Reverse transcription and PCR amplification were used to clone RGS4 from rat brain RNA using the following oligonucleotide primers: sense, 5'-CTGGATGAATTCGCCGCCACCATGTGCAAAGGACTCGCTGGTC-3'; antisense, 5'-CTGGATTCTAGACGGTCTCTGCCTCTGTGTGAGAATT-3'.

The PCR product was cut with *EcoRI* and *XbaI* and cloned into the pcDNA3.1(+) plasmid (Invitrogen). The entire nucleotide sequence of the cloned insert was verified (California Institute of Technology DNA Sequencing Facility) as identical to rat brain RGS4 (GenBank accession no. U27767). Following initial studies on the effects of RGS4, cDNAs for human RGS1, RGS2, and RGS3 (kindly provided by K. Druey and J. Kehrl, National Institutes of Health) were subsequently examined.

Oocyte Electrophysiology. Stage V and VI oocytes from *Xenopus laevis* were injected with various combinations of cRNAs synthesized *in vitro* (Ambion, Austin, TX) from linearized plasmids containing cDNAs for the m_2 receptor (provided by E. Peralta, Harvard University), the serotonin (5-

Abbreviations: RGS protein, regulator of G protein signaling; GIRK, G protein-gated inward rectifier K^+ ; GAP, GTPase-activating protein; β_2 -AR, β_2 -adrenergic receptor; ACh, acetylcholine; 5-HT, serotonin; CHO, Chinese hamster ovary; PLC- β_1 , phospholipase C- β_1 .

*Present address: Department of Physiology and Biophysics, University of South Florida, Tampa, FL 33612. e-mail: cdoupnik@com1.med.usf.edu.

†e-mail: davidsonn@starbase1.caltech.edu.

‡To whom reprint requests should be addressed. e-mail: lester@caltech.edu.

The publication costs of this article were defrayed in part by page charge payment. This article must therefore be hereby marked “advertisement” in accordance with 18 U.S.C. §1734 solely to indicate this fact.

© 1997 by The National Academy of Sciences 0027-8424/97/9410461-6\$2.00/0 PNAS is available online at <http://www.pnas.org>.

HT)_{1A} receptor (provided by P. Hartig, Synaptic Pharmaceutical), the Kir3.1 subunit (16), the Kir3.2 subunit (17), the Kir3.4 subunit (provided by J. Adelman, Oregon Health Sciences University), the β_2 -adrenergic receptor (β_2 -AR) (provided by B. Kobilka, Stanford University), the G α s subunit (provided by M. Simon, California Institute of Technology), and the RGS isoforms. For most experiments, oocytes were injected (final volume 50 nl) with 0.5 ng cRNA each for the m₂ receptor, Kir3.1, and Kir3.2, with and without the addition of 10 ng of RGS cRNA. For the β_2 -AR experiments, 0.5 ng of β_2 -AR and 5 ng G α s cRNAs were included (22). Injected oocytes were maintained overnight at 19°C in the following solution: 96 mM NaCl, 2 mM KCl, 1 mM CaCl₂, 1 mM MgCl₂, 5 mM Hepes, 2.5 mM sodium pyruvate, 0.5 mM theophylline, 50 μ g/ml gentamicin (pH 7.5).

Two-electrode voltage clamping of *Xenopus* oocytes was performed the day after cRNA injection as described in detail (18). The holding potential was -80 mV, and inward GIRK currents were recorded in a solution composed of 20 mM KCl, 78 mM NaCl, 1 mM MgCl₂, and 5 mM Hepes at pH 7.5. A U-tube superfusion apparatus was used to minimize agonist application and washout times. Analysis of the GIRK current kinetics was performed using PCLAMP 6.0 software.

Mammalian Cell Culture and cDNA Transfection. Adult rat atrial myocytes were isolated as described (19). Atrial cells and CHO-K1 cells (American Type Culture Collection) were plated in 35-mm dishes and grown in α -MEM supplemented with 5% fetal bovine serum and 100 units/ml penicillin and 100 μ g/ml streptomycin. For transfection of CHO-K1 cells, lipofectamine (GIBCO, 3 μ l per dish) was mixed with the following cDNAs cloned in the mammalian expression vector pcDNA3.1(+) (Invitrogen): 0.2 μ g m₂ receptor, 0.2 μ g Kir3.1, 0.2 μ g Kir3.2, and in some cases 0.2 μ g RGS4. In all cases, 0.1

μ g green fluorescent protein cDNA (GIBCO) was included as a reporter. CHO cells were then incubated in serum-free media Opti-MEM1 (GIBCO) for 16–18 h. Electrophysiological recordings from CHO cells were made 24–36 h from the start of the transfection on green fluorescent protein positive cells.

Electrophysiological Recording from Mammalian Cells.

Currents were recorded using the whole-cell voltage clamp configuration (20). Pipettes were pulled from borosilicate glass and fire-polished to a final resistance of 3–5 M Ω . Solution exchanges were accomplished with a DAD-12 perfusion system (Adams and List, Westbury, NY) with a time constant of 100 ms. Voltage protocols were generated and the data were digitized, recorded, and analyzed using PCLAMP 6.0 (Axon Instruments, Foster City, CA). Junction potentials were uncorrected and amounted to <3 mV. The pipette solution contained 130 mM potassium aspartate, 20 mM KCl, 1 mM MgCl₂, 5 mM EGTA, 5 mM Hepes, 0.1 mM Na₂GTP, and 2.5 mM MgATP (pH 7.3) (with NaOH). The external solution contained 111.5 mM NaCl, 30.4 mM KCl, 1.8 mM CaCl₂, 0.53 mM MgCl₂, and 5 mM Hepes (pH 7.3). All recordings were made at 20–23°C.

RESULTS

RGS Proteins Accelerate GIRK Deactivation and Activation Kinetics.

ACh-evoked GIRK currents recorded from *Xenopus* oocytes expressing muscarinic m₂ receptors and Kir3.1/Kir3.2 channels [mimicking the probable heteromultimeric state of some native neuronal GIRK channels (17)] deactivate with a time course well described by a single time constant of \approx 20 s (Fig. 1). This time constant agrees with earlier measurements of Kir3.1/Kir3.4 channels [mimicking the heteromultimeric

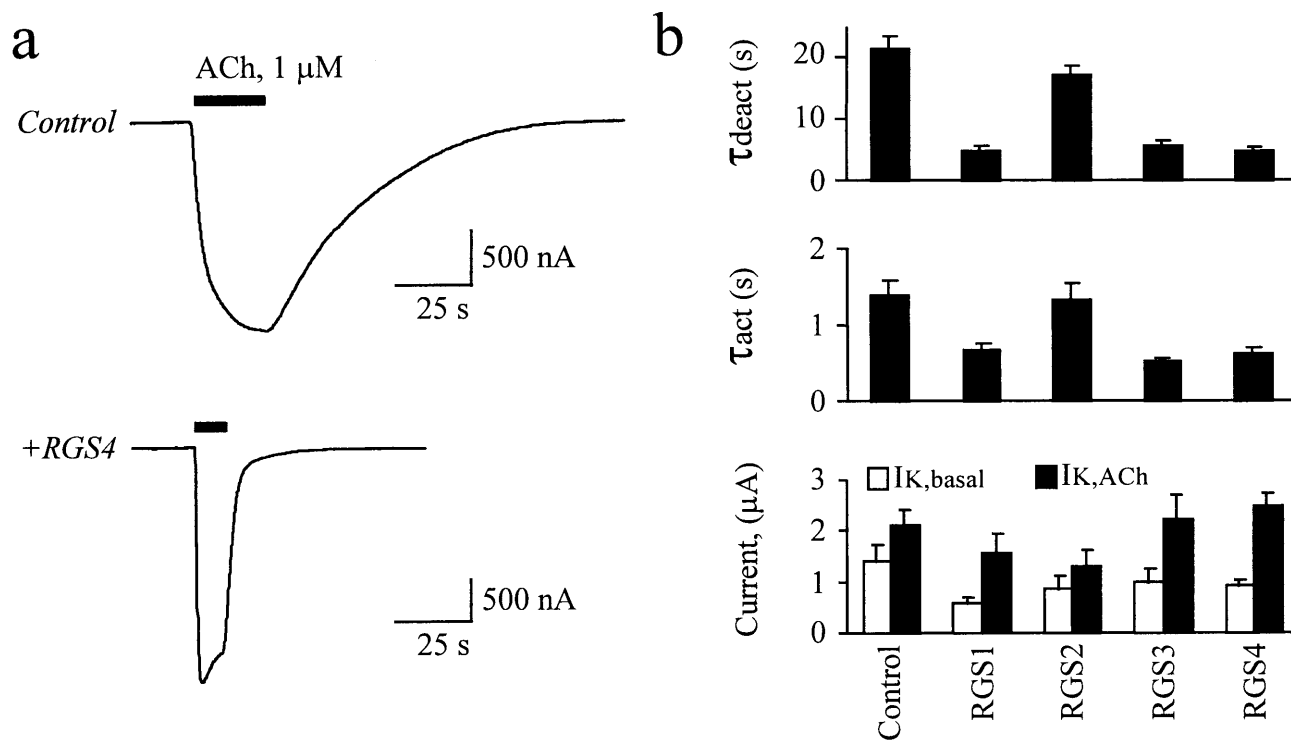


FIG. 1. Effects of RGS1–4 on the temporal and steady-state properties of m₂ receptor-evoked GIRK currents recorded from *Xenopus* oocytes. (a) Representative traces of ACh-evoked GIRK currents (Kir3.1/Kir3.2) recorded from oocytes not expressing (Control) or expressing RGS4 (+RGS4). (b) Top) Deactivation time constants (τ_{deact}) derived from exponential fits to the GIRK current deactivation phase from “Control” oocytes (i.e., not injected with RGS cRNA) or oocytes injected with cRNA (10 ng) for RGS1, RGS2, RGS3, or RGS4. (Middle) Activation time constants (τ_{act}) derived from exponential fits of the GIRK activation phase in oocytes expressing the various RGS proteins. (Lower) Effects of RGS proteins on “basal” GIRK currents ($I_{K,basal}$, open bars) measured as the inward current induced by changing the external [K⁺] from 0 to 20 mM. Solid bars are the amplitudes of inward GIRK currents induced by 1 μ M ACh ($I_{K,ACh}$) in 20 mM external [K⁺]. All bars are the mean \pm SEM from 12–15 oocytes from the same three batches.

state of atrial GIRK channels (14, 21)]. Coexpression of RGS1, RGS3, or RGS4 resulted in accelerated GIRK currents that rapidly deactivated (Fig. 1), with time constants of ≈ 4 s. RGS2, however, had no significant effect on the GIRK current waveform.

Interestingly, the time course for GIRK activation was also briefer in oocytes expressing RGS1, RGS3, or RGS4, but not RGS2 (Fig. 1). The GIRK activation rate was affected to a similar extent for the three effective RGS proteins, being ≈ 2 -fold faster than control or RGS2-expressing oocytes (Fig. 1*b*); however, the measurements may be limited by the time for solution change ($\tau \approx 1$ s). Associated with the RGS-accelerated GIRK activation phase was a significant decay of the current (i.e., desensitization) during a brief (10 s) agonist pulse (Fig. 1). If such desensitization also occurs in the absence of RGS, it would be obscured by the slow rise time of the responses. Although we did not systematically examine the effects of RGS expression on GIRK desensitization, experiments using longer agonist applications indicated that the rate and extent of desensitization on a time scale of minutes were not significantly affected by RGS expression. RGS4 similarly affected the activation and deactivation time courses of expressed Kir3.1/Kir3.4 channels, suggesting that the kinetic effects of RGS proteins do not depend strongly on GIRK subunit composition (data not shown).

RGS Proteins Suppress "Basal" GIRK Activity. Coexpression of RGS proteins did not significantly affect the amplitude of ACh-evoked GIRK currents ($I_{K,ACh}$), although the large variations among oocytes may have hidden subtle effects of RGS expression (Fig. 1*b*). Agonist independent "basal" GIRK currents ($I_{K,basal}$), however, were significantly reduced by RGS1 and RGS4 (Fig. 1*b*). For RGS1, $I_{K,basal}$ was reduced nearly 60% (control: $-1.40 \pm 0.32 \mu A$, +RGS1: $-0.57 \pm 0.12 \mu A$; mean \pm SEM, $n = 14$ oocytes paired from three different batches). For RGS4, $I_{K,basal}$ was reduced $\approx 42\%$ (control: $-1.26 \pm 0.24 \mu A$, +RGS4: $-0.73 \pm 0.11 \mu A$; mean \pm SEM, $n = 22$ -23 oocytes paired from five different batches).

RGS4 Does Not Affect the ACh Dose-Response Relation. The effects of RGS4 on m_2 receptor-evoked GIRK currents were examined over a wide range of ACh concentrations (10^{-9} to 10^{-5} M) (Fig. 2). GIRK deactivation time constants were roughly constant for currents evoked over the entire concentration range, and RGS expression reduced these time constants by 5- to 10-fold, with no systematic concentration dependence. As expected, the GIRK activation time constant was dependent on ACh concentration, and RGS4 reduced the time constant by roughly 2-fold at all concentrations (Fig. 2). Surprisingly, the steady-state ACh dose-response relation for GIRK current activation was not altered by coexpression of RGS4 (Fig. 2); the EC_{50} value for ACh was ≈ 50 nM, with or without RGS4 expression.

G α Subunit and Receptor Specificity. RGS1 and RGS4 do not affect the GTPase rate of G α s subunits *in vitro* (4-6). To test the G α specificity of the RGS effect on GIRK kinetics, we examined the effects of RGS4 on GIRK currents activated by a coexpressed G α s-coupled receptor, the β_2 -AR (22). In oocytes coexpressing both the m_2 receptor and β_2 -AR, RGS4 expression markedly accelerated ACh-evoked GIRK responses, both in the activation phase (by ≈ 2 -fold) and the deactivation phase, as in oocytes not expressing the β_2 -AR (cf. Fig. 2). There was no significant effect on the activation time course for the β_2 -AR-evoked currents. The deactivation time course of isoproterenol-evoked GIRK currents (Fig. 3) was only slightly briefer. Interestingly, the deactivation time course of isoproterenol-evoked GIRK currents displayed a significant lag phase prior to the current decay (22). The small but significant shortening of the isoproterenol-evoked GIRK deactivation by RGS4 may arise from one of two mechanisms that are consistent with a specific action of RGS4 on G $\alpha(i/o)$. (i) An increased G $\alpha(i/o)$ subunit GTPase rate in the absence

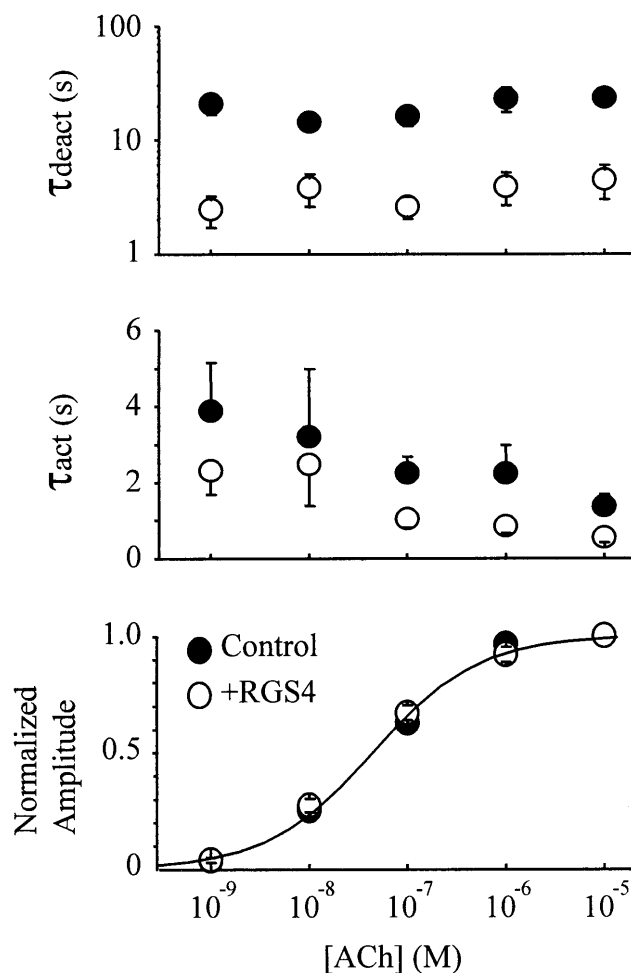


FIG. 2. ACh dose-effect relations for kinetic and steady-state GIRK gating properties. (Top) Deactivation time constants derived from exponential fits to the GIRK currents after washout of various ACh concentrations. Solid circles are values without RGS4 expression; open circles are with RGS4 expression (mean \pm SEM from four oocytes of the same batch). (Middle) Activation time constant of ACh-evoked GIRK currents as a function of ACh concentration with (open circle) and without (solid circle) coexpression of RGS4. The time course for GIRK activation was fit with an exponential function plus a sloping base line. (Lower) Steady-state ACh dose-response curve for GIRK responses with (open circles) and without (solid circles) RGS4 expression. Current amplitudes were normalized to the currents evoked by $10 \mu M$ ACh for each cell (1 - $2 \mu A$) and are from the same records used to derive the kinetic data shown in Top and Middle. The data (solid circles) were fitted with a Hill function (solid line) having an EC_{50} value of 48 nM.

of m_2 R activation is inferred from the RGS4-mediated reduction in basal GIRK activity (see Fig. 1). This implies a raised level of G $\alpha(i/o)$ -GDP, which would be available to sequester G $\beta\gamma$ from β_2 -AR-activated GIRK channel, thereby promoting faster deactivation. (ii) β_2 -ARs might activate GIRK channels in part via promiscuous coupling to G $\alpha(i/o)$.

To test whether the RGS isoforms differentially affected GIRK channels activated by a different G $\alpha(i/o)$ -coupled receptor, we examined the effects of RGS1-4 on 5-HT-evoked GIRK currents in oocytes coexpressing the 5-HT $_{1A}$ receptor together with the m_2 receptor. In data not shown, 5-HT-evoked GIRK currents showed RGS-mediated effects and a profile (i.e., accelerated activation and deactivation by RGS1, RGS3, and RGS4) resembling the data for the ACh-evoked GIRK currents, indicating that RGS proteins show no specificity between m_2 receptors and 5-HT $_{1A}$ receptors.

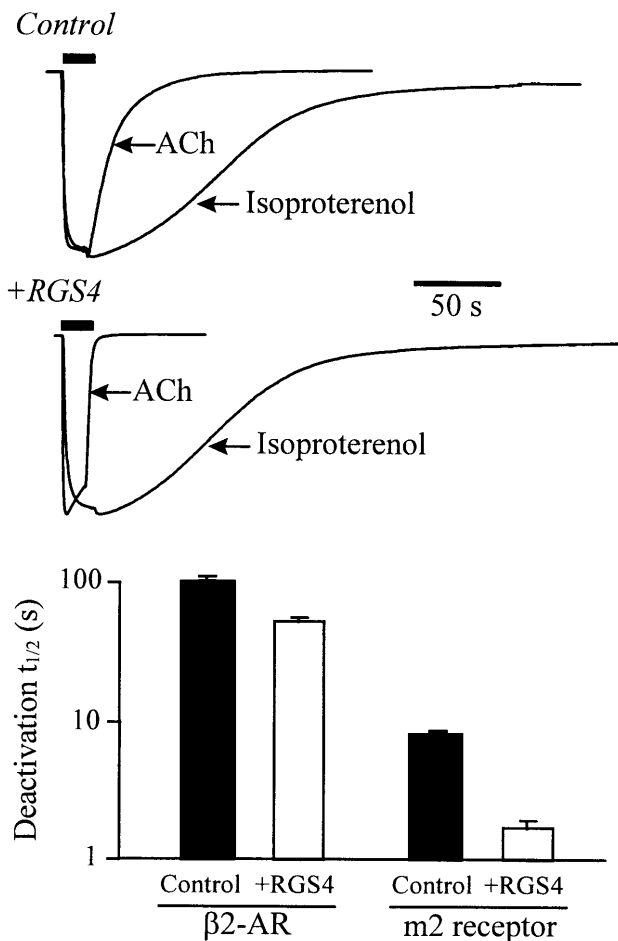


FIG. 3. RGS4 selectively accelerates the gating of $G\alpha(i/o)$ receptor-coupled GIRK currents. *Xenopus* oocytes coexpressing the m_2 receptor, β_2 -AR, $G\alpha_s$, Kir3.1, and Kir3.2 elicit GIRK currents in response to either ACh (1 μ M) or isoproterenol (1 μ M). (Upper) Superimposed ACh- and isoproterenol-evoked GIRK current records are from the same oocyte either expressing (+RGS4) or not expressing RGS4 (Control), and have been normalized for comparison. (Lower) Summary of the deactivation half times ($t_{1/2}$) for ACh-evoked and β_2 -AR-evoked GIRK currents with (open bar) and without (solid bar) RGS4 coexpression. (Bars are the mean \pm SEM from 6–10 oocytes from two batches of oocytes.)

RGS4-Accelerated GIRK Currents Mimic Native GIRK Current Kinetics. We also examined the effects of RGS4 cotransfected into CHO-K1 cells with the m_2 receptor, Kir3.1, and Kir3.2 (Fig. 4). For these experiments we used a superfusion system capable of changing external solutions with a time constant of <100 ms, compared with the possibly limiting exchange rate in the oocyte experiments ($\tau \approx 1$ –2 s). In cells not expressing RGS4, the ACh-evoked currents deactivated with time constants of ≈ 9 s (Fig. 4a); in cells cotransfected with RGS4, the deactivation time constants ranged from 0.5 to 1 s. Moreover, with RGS4 present, the GIRK deactivation rates were equivalent to the deactivation rates of native GIRK current recorded from cultured rat atrial cells (Fig. 4a).

For the GIRK activation phase with coexpressed RGS4, a brief lag time (<50 ms) followed by a time constant <1 s (Fig. 4b) closely matches the activation time course for atrial muscarinic responses (23, 24) and γ -aminobutyric acid type B responses in hippocampal neurons (13). The activation rate was agonist dependent and accelerated by RGS4 to an extent similar to that observed in oocytes (Fig. 4b). ACh dose-response relations yielded an EC_{50} value of ≈ 300 nM in the presence of RGS4, which agreed within 2-fold with measurements in the absence of RGS4 (data not shown).

Effect of RGS Expression on GIRK Currents Evoked by Brief Agonist Pulses. The consequences of the RGS accelerated kinetics for physiologically relevant brief agonist applications are illustrated in an experiment on CHO cells (Fig. 5). The duration of ACh application was varied from 1 to 20 s. With RGS4 expression, a 1-s application of 1 μ M ACh leads to full activation of the GIRK current. Without RGS4 expression, a 1-s application leads to a smaller amplitude but much prolonged GIRK current waveform. Because of the accelerated deactivation phase, the integrated K^+ current (charge movement) that flows for the 1 s application is $\approx 50\%$ less with RGS4 coexpression, reminiscent of the negative regulation described for the yeast pheromone pathway (2, 25) and for egg-laying behavior in *Caenorhabditis elegans* (3). These experiments emphasize that for a brief agonist application, such as during a single synaptic event, RGS4 would increase the peak amplitude of GIRK currents in addition to accelerating the decay phase upon removal of transmitter.

DISCUSSION

RGS Specificity and GIRK Channel Kinetics. The results of this study demonstrate that coexpression of certain RGS proteins (i.e., RGS1, RGS3, or RGS4) with GIRK channels and $G\alpha i/o$ -coupled receptors reconstitutes the rapid gating characteristics of native atrial and neuronal GIRK currents. Northern blot analysis indicates that RGS3 and RGS4 are highly expressed in the heart and brain, respectively (2, 3), and therefore are candidates for conferring the rapid kinetics of atrial and neuronal GIRK channels. RGS1 on the other hand, which was as effective as RGS3 and RGS4 in accelerating GIRK currents in *Xenopus* oocytes, is a mitogen-activated immediate-early gene expressed in B lymphocytes and not detected in the heart or brain (26). RGS2, also an immediate-early gene expressed in malignant hematopoietic and nonhematopoietic cells (27), had no significant effect on GIRK current waveforms. Recent experiments show that RGS2 does not interact with $G\alpha i2$, $G\alpha i3$, or $G\alpha o$ subunits *in vitro* under conditions (i.e., GDP-AIF₄) that favor binding by RGS1, RGS3, and RGS4 (28). Therefore, the lack of RGS2 effects on GIRK kinetics may be explained by an inability to interact effectively with $G\alpha i/o$ subunits. The effect of RGS1 on GIRK gating suggests that other RGS isoforms expressed in the heart and brain (i.e., GAIP, RGS5, RGS7, RGS10), which interact effectively with $G\alpha i/o$ proteins, might also be expected to accelerate GIRK channel gating.

Kinetic Anomalies Associated with RGS-Accelerated GIRK Currents. In both *Xenopus* oocytes and CHO cells expression of RGS4 dramatically accelerated GIRK activation as well as deactivation. According to classical kinetic concepts, the accelerated GIRK activation time course could occur even if the only kinetic process(es) altered by RGS4 expression is the deactivation of the GIRK conductance upon removal of the agonist. We therefore analyzed the macroscopic GIRK activation and deactivation rates to ascertain whether the process(es) governing activation was affected to the same extent as that for deactivation. Formally, we assumed a simple two-state model (closed and open), where the rate constant for GIRK current activation ($1/\tau_{act}$) is equal to the sum of the macroscopic opening and closing rate constants, k_{open} and k_{close} , respectively. The parameter k_{open} is expected to depend on the agonist concentration; and the deactivation rate ($1/\tau_{deact}$) gives k_{close} , which is measured upon agonist removal. Because the macroscopic GIRK current relaxations are much slower than the lifetime of single-channel openings (0.5 to 3.5 ms) (17), k_{open} and k_{close} represent multistep processes that are thought to control complex bursts of GIRK channel activity (29). When these relations were used to calculate k_{open} , we found that RGS4 expression had no effect on the GIRK opening rate k_{open} in transfected CHO cells and only a 2-fold

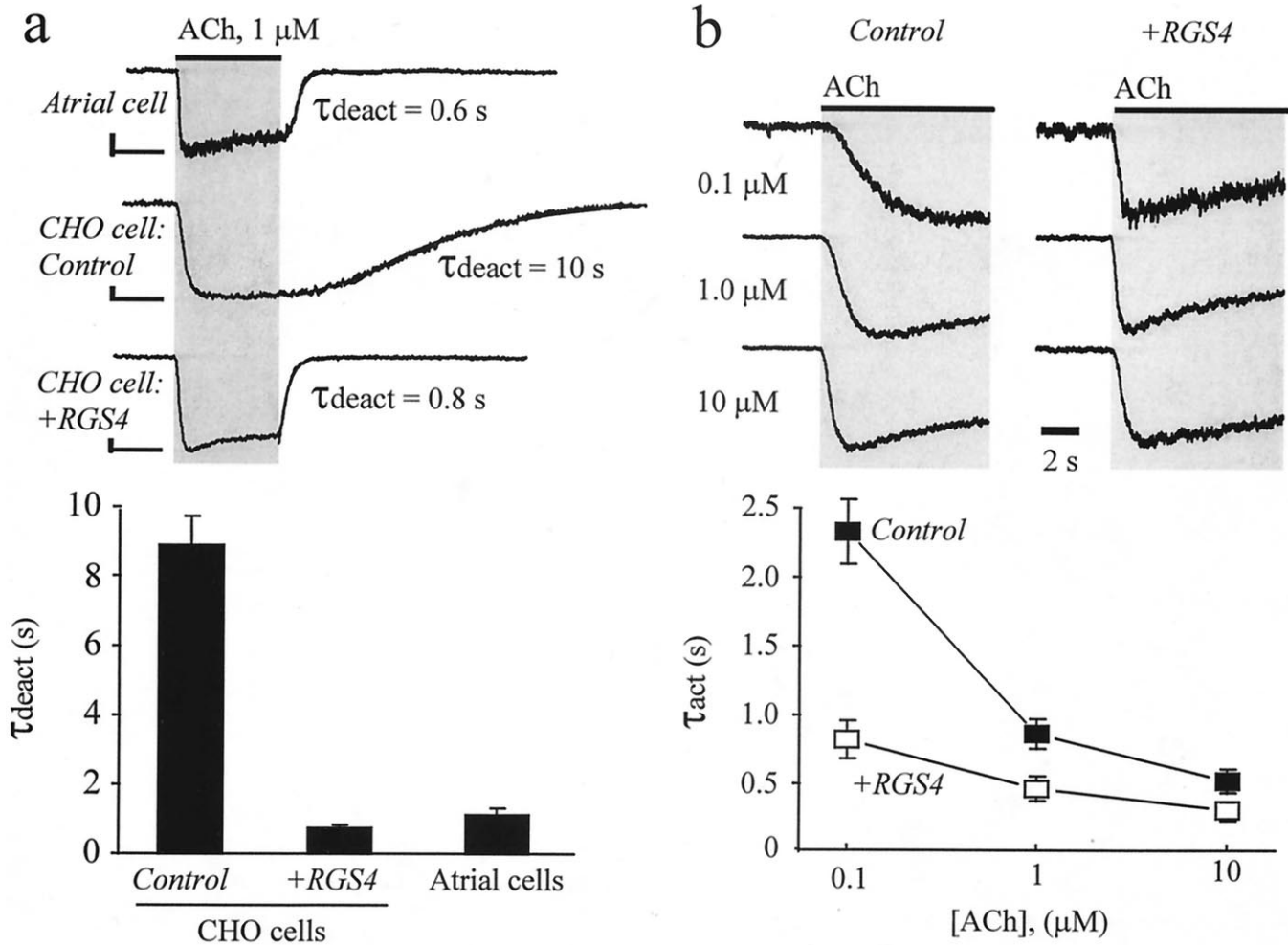


FIG. 4. RGS4 expression in GIRK-transfected CHO cells elicits currents that mimic native atrial GIRK currents in their temporal gating properties. (a Upper) Current traces from a rat atrial myocyte and from CHO cells transfected with the m_2 receptor, Kir3.1, Kir3.2, and without (control) or with (+RGS4) RGS4 cDNA. ACh (1μ M) was applied for 10 s. The time constant for solution changes was <100 ms. (Scale bars = 200 pA and 5 s.) Exponential fits to the current deactivation were used to derive τ_{deact} . (Lower) Deactivation time constants (τ_{deact}) for atrial ($n = 6$) and CHO cells transfected with ($n = 22$) or without ($n = 23$) RGS4. (Bars = mean \pm SEM.) (b Upper) Activation phase of current traces for cells exposed to increasing concentrations of ACh. Current amplitudes were normalized to the currents evoked at 10μ M ACh. (Lower) Summary of the GIRK activation time constant (τ_{act}) as a function of ACh concentration obtained from at least four cells without (control) and with RGS4 coexpression (mean \pm SEM). The holding potential was -80 mV.

increase in oocytes, in comparison with the 10- to 20-fold increase in k_{close} for both expression systems. This initial analysis suggests that the accelerated GIRK activation rate is

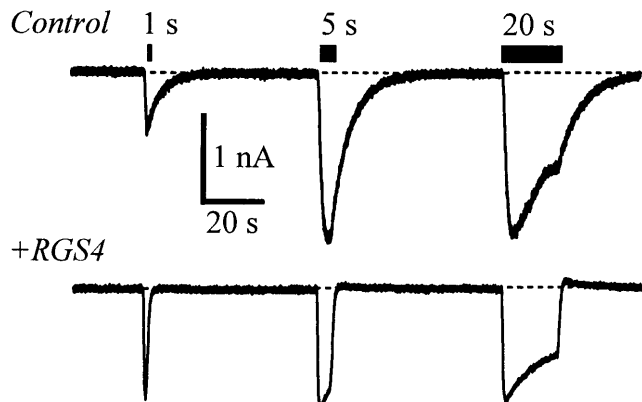


FIG. 5. Effects of RGS4 on GIRK current waveforms produced by varying durations of m_2 receptor activation. Current traces from transfected CHO cells are as described in Fig. 4, exposed to 1μ M ACh for 1, 5, and 20 s. Holding potential, -80 mV.

due primarily to the accelerated closing rate. Yet this conclusion is confounded by the prediction that a greater k_{close} , with unchanged k_{open} , would produce a profound reduction in steady-state current amplitudes and a shift in the ACh dose-response curve, which were not observed experimentally.

These kinetic anomalies are reminiscent of those encountered with the muscarinic m_1 receptor-Gq-phospholipase C- β_1 (PLC- β_1)-signaling pathway that arise from the GTPase activity of PLC- β_1 (8, 30). A "quasi-stable" receptor-G protein-effector complex has been proposed for this system (8, 30), allowing Gq subunits to undergo multiple GTPase cycles while associated with both receptor and effector (PLC- β_1). This molecular configuration favors an accelerated receptor-catalyzed GDP \rightarrow GTP exchange rate that is dependent on the GTPase activity of PLC- β_1 , and permits otherwise unattainable steady-state levels of effector activation. Biochemical evidence demonstrating the association of $G\alpha(GDP)\beta\gamma$ heterotrimers with the amino terminal domain of the Kir3.1 subunit (31) suggests the existence of an analogous m_2 receptor-G protein-GIRK channel complex (31, 32), of which RGS proteins may be an important participant. The value for k_{open} was not increased by RGS4, consistent with the view that this parameter is governed by the rate of receptor-catalyzed GDP

→ GTP exchange (3). Although RGS4 does not affect the GDP → GTP exchange rate for G α (i/o) subunits *in vitro* (4), its effect in the presence of activated receptors and effectors has not yet been determined. We suggest that the discrepancy between the kinetic and steady-state data provides functional evidence for a complex among the m₂ receptor, G α , RGS4, G $\beta\gamma$, and the GIRK channel (31, 32).

Molecular Mechanisms Involved in GIRK Channel Gating. G $\beta\gamma$ dimers directly interact with both the Kir3.1 and Kir3.4 channel subunits (14, 31, 33, 34) that comprise the atrial GIRK channel (21). These binding events are thought to activate the channel by stabilizing an open-state conformation(s). G α subunits also bind to GIRK subunits (31, 34), but do not activate GIRK channels (12, 35) and in some cases inhibit instead (36). The observations that RGS proteins accelerate both GTP hydrolysis (4–6) and GIRK channel deactivation provide strong support for the proposal that the deactivation rate is determined by the GTP hydrolysis rate of G α (i/o) subunits (11), and not by the much slower intrinsic rate of G $\beta\gamma$ dissociation from the GIRK channel (≤ 0.003 s⁻¹ at 25°C, even slower at 4°C) (14, 33). Perhaps the accelerated deactivation involves interactions between G α -GDP and G $\beta\gamma$ subunits when both are directly bound to the channel, leading to sequestration of G $\beta\gamma$ more rapidly than would be provided by intrinsic G $\beta\gamma$ dissociation (12).

CONCLUSIONS

In our time-resolved measurements, RGS proteins exert an effect on a G $\beta\gamma$ effector (GIRK channels) that is primarily kinetic, complementing and extending the observations of negative regulation described for the yeast pheromone pathway (2, 25) and for egg-laying behavior in *C. elegans* (3). Responses to G protein-coupled receptors are generally classified as “neuromodulatory” processes that provide a means of “tuning” membrane excitability in response to specific input stimuli (37). A large number of receptors in the nervous system are coupled to Gai/o pathways; and the present results show how G α (i/o) $\beta\gamma$ -coupled receptors can, with the aid of RGS proteins, rapidly activate channels (and presumably other effectors) and then rapidly deactivate them as well. These temporal signaling properties are essential for establishing the time course of GIRK-mediated hyperpolarizing postsynaptic potentials that underlie certain forms of inhibitory synaptic transmission (38, 39). It will be important to know how distinct G α (i/o)-coupled responses to specific receptors and effectors (i.e., Ca²⁺ channels) are shaped by individual members of the growing RGS protein family.

We thank Drs. Kirk Druey and John Kehrl for providing RGS1–3 cDNAs, Brad Henkle and Hai-Rong Li for preparing oocytes, and Dr. Mark Jasek for helping with the mammalian cell transfection procedures. This work was supported by fellowships from the American Heart Association (C.A.D. and P.K.) and the Guenther Foundation (P.K.), and by grants from the National Institutes of Health and the National Institute of Mental Health.

1. De Vries, L., Mousli, M., Wurmser, A. & Farquhar, M. G. (1995) *Proc. Natl. Acad. Sci. USA* **92**, 11916–11920.
2. Druey, K. M., Blumer, K. J., Kang, V. H. & Kehrl, J. H. (1996) *Nature (London)* **379**, 742–746.
3. Koelle, M. R. & Horvitz, H. R. (1996) *Cell* **84**, 115–125.
4. Berman, D. M., Wilkie, T. M. & Gilman, A. G. (1996) *Cell* **86**, 445–452.

5. Watson, N., Linder, M. E., Druey, K. M., Kehrl, J. H. & Blumer, K. J. (1996) *Nature (London)* **383**, 172–177.
6. Hunt, T. W., Fields, T. A., Casey, P. J. & Peralta, E. G. (1996) *Nature (London)* **383**, 175–177.
7. Dohlman, H. G. & Thorner, J. (1997) *J. Biol. Chem.* **272**, 3871–3874.
8. Ross, E. M. (1995) *Recent Prog. Horm. Res.* **50**, 207–221.
9. Gilman, A. G. (1987) *Annu. Rev. Biochem.* **56**, 615–649.
10. Chen, C.-K., Wieland, T. & Simon, M. I. (1996) *Proc. Natl. Acad. Sci. USA* **93**, 12885–12889.
11. Breitwieser, G. E. & Szabo, G. (1988) *J. Gen. Physiol.* **91**, 469–494.
12. Kurachi, Y. (1995) *Am. J. Physiol.* **38**, C821–C830.
13. Soddickson, D. L. & Bean, B. P. (1996) *J. Neurosci.* **16**, 6374–6385.
14. Doupnik, C. A., Dessauer, C. W., Slepak, V. Z., Gilman, A. G., Davidson, N. & Lester, H. A. (1996) *Neuropharmacology* **35**, 923–931.
15. Shui, Z., Boyett, M. R., Zang, W. J., Haga, T. & Kameyama, K. (1995) *J. Physiol. (London)* **487.2**, 359–366.
16. Dascal, N., Schreibleymer, W., Lim, N. F., Wang, W., Chavkin, C., DiMugno, L., Labarca, C., Kieffer, B. L., Gaveriaux-Ruff, C., Trollinger, D., Lester, H. A. & Davidson, N. (1993) *Proc. Natl. Acad. Sci. USA* **90**, 10235–10239.
17. Kofuji, P., Davidson, N. & Lester, H. A. (1995) *Proc. Natl. Acad. Sci. USA* **92**, 6542–6546.
18. Doupnik, C. A., Lim, N. F., Kofuji, P., Davidson, N. & Lester, H. A. (1995) *J. Gen. Physiol.* **106**, 1–23.
19. Karschin, A., Ho, B., Labarca, C., Elroy-Stein, O., Moss, B., Davidson, N. & Lester, H. A. (1991) *Proc. Natl. Acad. Sci. USA* **88**, 5694–5698.
20. Hamill, O. P., Marty, A., Neher, E., Sakmann, B. & Sigworth, F. J. (1981) *Pflügers Arch.* **391**, 85–100.
21. Krapivinsky, G., Gordon, E. A., Wickman, K., Velimirovic, B., Krapivinsky, L. & Clapham, D. E. (1995) *Nature (London)* **374**, 135–141.
22. Lim, N. F., Dascal, N., Labarca, C., Davidson, N. & Lester, H. A. (1995) *J. Gen. Physiol.* **105**, 421–439.
23. Pott, L. & Pusch, H. (1979) *Pflügers Arch.* **383**, 75–77.
24. Nargeot, J., Lester, H. A., Birdsall, N. J. M., Stockton, J., Wassermann, N. H. & Erlanger, B. F. (1982) *J. Gen. Physiol.* **79**, 657–678.
25. Dohlman, H. R., Apaniesk, D., Chen, Y., Song, J. P. & Nusskern, D. (1995) *Mol. Cell. Biol.* **15**, 3635–3643.
26. Hong, J. X., Wilson, G. L., Fox, C. H. & Kehrl, J. H. (1993) *J. Immunol.* **150**, 3895–3904.
27. Wu, H.-K., Heng, H. H. Q., Shi, X.-M., Forsdyke, D. R., Tsui, L.-C., Mak, T. W., Minden, M. D. & Siderovski, D. P. (1995) *Leukemia* **9**, 1291–1298.
28. Chen, C., Zheng, B., Han, J. & Lin, S.-C. (1997) *J. Biol. Chem.* **272**, 8679–8685.
29. Ivanova-Nikolova, T. T. & Breitwieser, G. E. (1997) *J. Gen. Physiol.* **109**, 245–253.
30. Biddlecome, G. H., Berstein, G. & Ross, E. M. (1996) *J. Biol. Chem.* **271**, 7999–8007.
31. Huang, C.-L., Slesinger, P. A., Casey, P. J., Jan, Y. N. & Jan, L. Y. (1995) *Neuron* **15**, 1133–1143.
32. Slesinger, P. A., Reuveny, E., Jan, Y. N. & Jan, L. Y. (1995) *Neuron* **15**, 1145–1156.
33. Krapivinsky, G., Krapivinsky, L., Wickman, K. & Clapham, D. E. (1995) *J. Biol. Chem.* **270**, 29059–29062.
34. Kunkel, M. T. & Peralta, E. G. (1995) *Neuron* **83**, 443–449.
35. Wickman, K. D., Inlguez-Lluhl, J. A., Davenport, P. A., Taussig, R., Krapivinsky, G. B., Linder, M. E., Gilman, A. G. & Clapham, D. E. (1994) *Nature (London)* **368**, 255–257.
36. Schreibleymer, W., Dessauer, C. W., Vorobiov, D., Gilman, A. G., Lester, H. A., Davidson, N. & Dascal, N. (1996) *Nature (London)* **380**, 624–627.
37. Hille, B. (1992) *Ionic Channels in Excitable Membranes* (Sinauer, Sunderland, MA).
38. Nicoll, R. A. (1988) *Science* **241**, 545–551.
39. North, R. A. (1989) *Br. J. Pharmacol.* **98**, 13–28.